



Animal cell invasion by a large nonenveloped virus: reovirus delivers the goods

Kartik Chandran and Max L. Nibert

Department of Microbiology and Molecular Genetics, Harvard Medical School, 200 Longwood Avenue, Boston, MA 02115, USA

Molecular mechanisms by which nonenveloped animal viruses penetrate a cellular membrane to invade the host cytoplasm remain less well characterized than those used by enveloped viruses. Mammalian reoviruses are useful agents for addressing this problem, especially in light of recent crystal structure determinations for the viral proteins and development of a new genetic tool with which to dissect the viral determinants of cell invasion. The roles of penetration protein $\mu 1$ and its protector protein $\sigma 3$ are beginning to come into focus.

The infectious particles of animal viruses could be conceptually divided into two modules: (1) payload, the nucleic acid or nucleoprotein complex that must gain access to the cytoplasm for replication to proceed, and (2) delivery system, the machinery that encloses and protects the payload and mediates its transfer into the cytoplasm [1]. Animal viruses are categorized as enveloped or nonenveloped based on the nature of their delivery systems. Enveloped viruses possess a cell-derived lipid bilayer (envelope) in which are anchored multiple copies of a virus-encoded integral membrane protein, the fusion protein. This molecular machine mediates delivery of payload by promoting coalescence of viral and cellular lipid bilayers. Nonenveloped viruses lack a lipid bilayer and thus cannot use fusion as a mechanism for invasion. Instead of this, they contain multiple copies of one or more capsid proteins, the 'penetration protein(s)', which transfer payload into the cytoplasm, possibly by forming a discrete pore through, or by locally disrupting, a cellular bilayer.

Studies of membrane fusion, augmented by high-resolution structural data for pre- and/or post-fusion states of several fusion proteins (e.g. influenza virus HA and flavivirus E proteins) have provided a detailed understanding of how enveloped viruses invade cells [2–4]. When triggered by a host cell stimulus (e.g. low pH), the fusion protein complexes undergo major conformational changes and deploy a hydrophobic fusion peptide into the cellular bilayer, then rearrange further to promote apposition of viral and cellular bilayers. The apposed bilayers mix, forming a pore that expands to complete the fusion process. There are few restrictions to the size of

payload that can be introduced by this means, and, indeed, the payloads of enveloped viruses are commonly large nucleoprotein complexes.

Less is known about shared features of the non-enveloped virus penetration proteins, although several are modified by an N-terminal myristoyl (C_{14} acyl) group (e.g. orthoreovirus $\mu 1N$, poliovirus VP4, and polyomavirus VP2) and/or subject to autolytic cleavage (e.g. nodavirus $\alpha \rightarrow \beta + \gamma$, orthoreovirus $\mu 1 \rightarrow \mu 1N + \mu 1C$, and poliovirus VP0 \rightarrow VP4 + VP2) [3,5,6]. High-resolution structural data are available for some penetration proteins but only in their 'pre-penetration' states; hence, the nature of conformational changes during invasion remains poorly characterized. Furthermore, membrane-interacting sequences analogous to enveloped virus fusion peptides have yet to be identified for many of these proteins. Finally, only limited clues have emerged to explain the means by which payloads as distinct as a translatable RNA chain (e.g. nodavirus and poliovirus), a transcription-competent RNA–protein complex (e.g. orthoreovirus) or a nucleus-targeting DNA–protein complex (e.g. adenovirus) are translocated into the cytoplasm.

The mammalian orthoreoviruses (reoviruses) are prototypes of the large *Reoviridae* family of double-strand (ds) RNA viruses that also includes the clinically important rotaviruses [7,8]. These viruses are ubiquitous in nature and infect a wide range of mammals, including humans, most commonly by the fecal–oral route. In the remainder of this review, recent progress in understanding the structure and function of the reovirus delivery system will be discussed.

Organization and programmed disassembly of the outer capsid

Reovirus virions (Fig. 1) are large particles, ~ 85 nm in diameter, comprising a ten-segment dsRNA genome surrounded by eight proteins in two concentric icosahedral capsids (Table 1). The genome and five innermost proteins constitute a self-contained transcription unit, the 'core' or 'inner capsid' particle, that uses ribonucleoside triphosphates and *S*-adenosyl-L-methionine from the host cell to synthesize and export translatable viral mRNAs. This mRNA synthesis machine forms a major part of the payload. The three other proteins in virions – $\mu 1$, $\sigma 1$ and $\sigma 3$ – constitute the delivery system. They, along with core

Corresponding author: Max L. Nibert (mnibert@hms.harvard.edu).

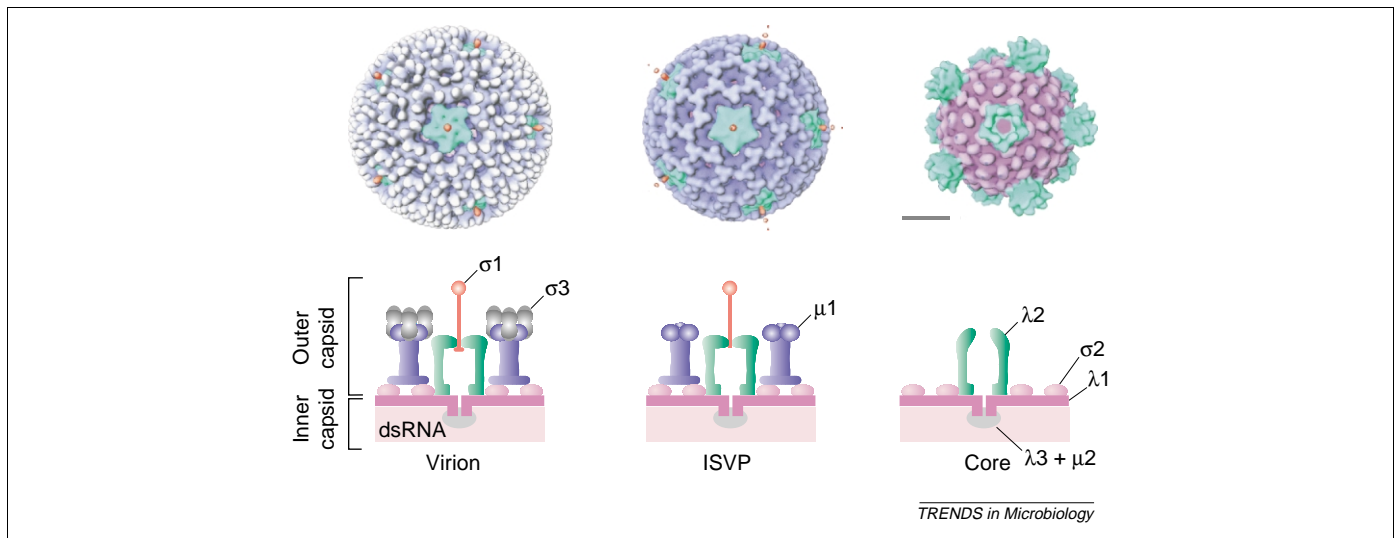


Fig. 1. Organization of virus particles. Upper row shows surface-shaded views of reovirus virion, intermediate subvirion particle (ISVP) and core obtained by transmission electron cryomicroscopy and three-dimensional image reconstruction [14]. Color coding of the capsid proteins was applied for clarity. Images are approximately to scale. Bar, 20 nm. Lower row shows schematic cross-sectional views of a portion of each particle. Proteins are color coded, as in the reconstructions, and labeled in a representative fashion. Diagrams are not to scale.

protein $\lambda 2$, are exposed on the virion surface, where they can fulfill their functions in cell invasion, and are thus analogous to the lipid bilayer and membrane glycoproteins of enveloped viruses. Protein $\lambda 2$ forms a pentameric turret around each icosahedral fivefold axis and adds a 5' cap to the viral mRNA as it passes through the turret's central cavity [9,10] (Fig. 2). The $\lambda 2$ turret also participates in conformational remodeling and disassembly of the outer capsid during invasion [11]. At the centre of each turret is anchored the base of a trimeric receptor-binding fiber of the adhesin $\sigma 1$ [11,12] (Figs. 1 and 2). The bulk of the outer capsid consists of 200 heterohexameric complexes of the penetration protein $\mu 1$ and its protector protein $\sigma 3$, arranged in a fenestrated $T = 13$ net over the $T = 1$ inner capsid [13] (Figs. 1 and 3). Contacts between $\mu 1$ and $\lambda 2$ around the fivefold axes and contacts among the $\mu 1$ trimers at other positions cement this net in place. The $\sigma 3$ subunits bound to the upper part of each $\mu 1$ trimer cover much of the $\mu 1$ surface and play a crucial role in regulating the activities of viral particles during their extracellular and invasive phases.

Reovirus virions undergo progressive disassembly when treated with proteases *in vitro*, generating several types of 'subvirion' particles that lack outer-capsid

proteins. The best known of these are intermediate subvirion particles (ISVPs) and cores (Fig. 1, Table 1). ISVPs have lost $\sigma 3$ to degradation and contain $\mu 1$ as the major surface protein. They remain highly infectious, indicating that $\sigma 3$ is not directly required for invasion. Cores additionally lack $\mu 1$ and $\sigma 1$ and contain an altered conformer of the $\lambda 2$ turret, in which the $\sigma 1$ anchoring site is disrupted. Unlike virions and ISVPs, cores are poorly infectious, suggesting that $\mu 1$ and $\sigma 1$ are important for infection. ISVPs and cores resemble particles that are generated during cell invasion and thought to play key roles in membrane penetration and viral mRNA synthesis, respectively [14]. The shedding of viral proteins during the course of invasion reflects the dynamic nature of this process.

New tools for studies of cell invasion

Both ISVPs and cores are suitable substrates for reassembling the reovirus outer capsid. Recent work has shown that recombinant $\sigma 3$ can bind in large amounts to purified ISVPs *in vitro*, regenerating the $\sigma 3$ coat [15]. Similarly, incubation of purified cores with recombinant $\mu 1$ and $\sigma 3$, together with recombinant $\sigma 1$, completely restores the outer capsid [11,16]. Remarkably, these 'recoated' particles

Table 1. Genome segments and proteins in reovirus particles

Gene segment	Encoded protein	Copy number	Location in particle ^a	Present in particle types ^b	Role in cell invasion	PDB ID ^c
L1	$\lambda 3$	12	Inner	V, I, I*, C	Transcription	1MUK
L2	$\lambda 2$	60	Outer	V, I, I*, C	mRNA capping	1EJ6
L3	$\lambda 1$	120	Inner	V, I, I*, C	Transcription	1EJ6
M1	$\mu 2$	24(?)	Inner	V, I, I*, C	Transcription	–
M2	$\mu 1$	600	Outer	V, I, I*	Membrane penetration	1JMU
M3	μNS	–	–	–	–	–
S1	$\sigma 1$	36	Outer	V, I	Cell adhesion	1KKE
S1	$\sigma 1s$	–	–	–	–	–
S2	$\sigma 2$	150	Inner	V, I, I*, C	?	1EJ6
S3	σNS	–	–	–	–	–
S4	$\sigma 3$	600	Outer	V	Penetration regulator	1JMU, 1FN9

^aInner or outer capsid.

^bV, virion; I, ISVP; I*, ISVP*; C, core.

^cPDB files can be downloaded or viewed at the Protein Data Bank website. (<http://www.rcsb.org/pdb>).

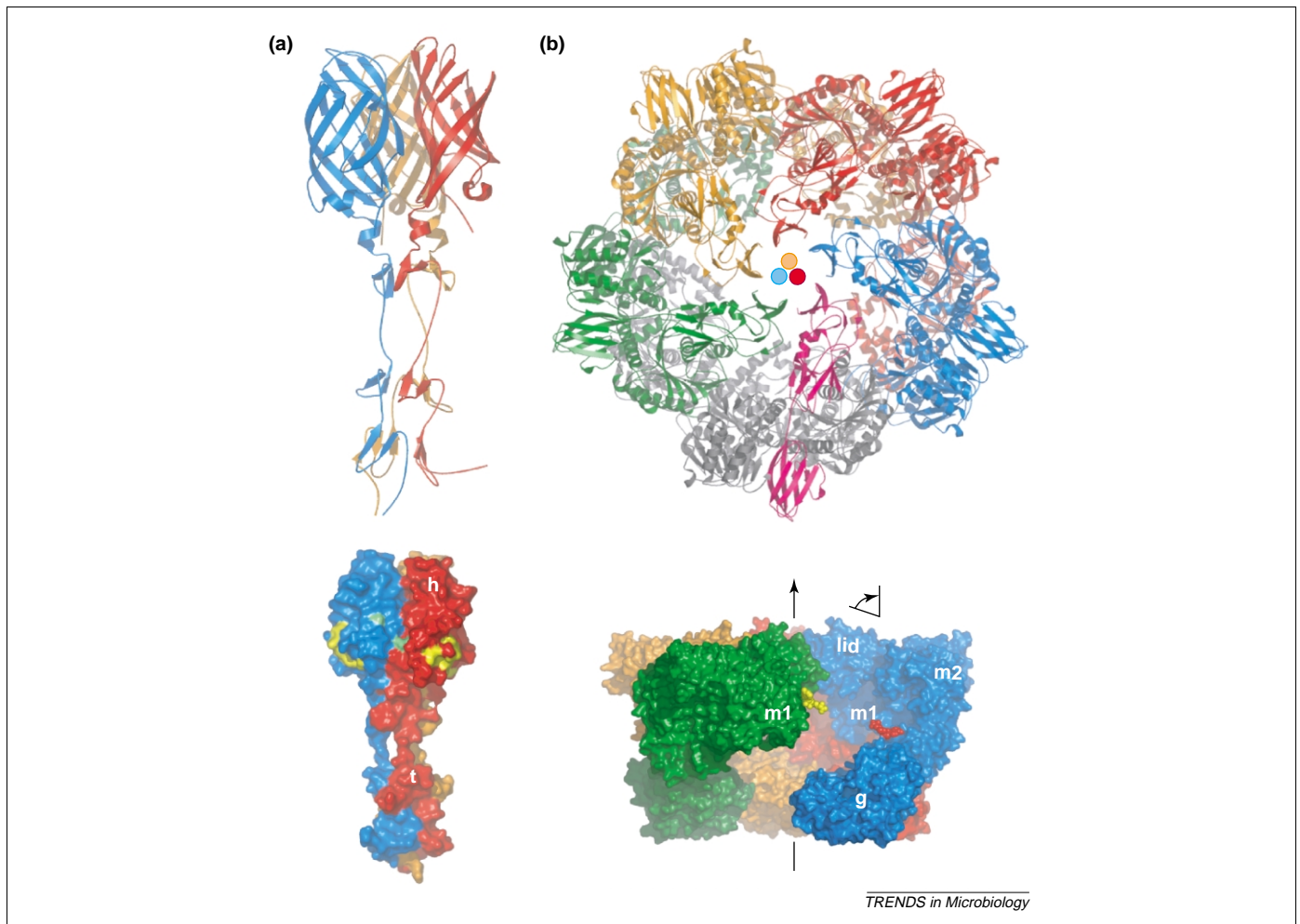


Fig. 2. Structural features of outer-capsid proteins $\sigma 1$ and $\lambda 2$. (a) Side view of a C-terminal portion (residues 250 to 455) of the trimeric $\sigma 1$ fiber [12] rendered as ribbon (top) and surface-shaded (bottom) models. Subunits are color coded in aquamarine, orange and red. Surface-shaded model is labeled to indicate the head (h), comprising a trimer of jelly roll β -barrels, and the tail (t), comprising four repeats of a triple β -spiral motif. Surface-exposed residues conserved in viral isolates representing all three established serotypes and proposed to participate in binding to cell surface receptor JAM1 [27,63] are color coded in yellow. Two residues whose mutations confer resistance to a $\sigma 1$ -specific neutralizing antibody are color-coded in green. (b) Top view of the pentameric $\lambda 2$ turret [9] rendered as a ribbon model (top). Four subunits are color coded in green, orange, red and aquamarine. The fifth is color coded in grey (residues 2 to 1032) and pink (residues 1033 to 1289) to highlight three immunoglobulin-like domains which form one cantilevered arm of the pentameric 'lid' that lies across the top of the turret. Residues within the outermost immunoglobulin-like domain are proposed to contact the base of the $\sigma 1$ trimer (aquamarine, orange and red circles) bound at the center of the turret in virions and intermediate subviral particles (ISVPs). At the bottom is a side view of the $\lambda 2$ turret (bottom of the top view has been rotated 90° toward the viewer) rendered as a surface-shaded model. Subunits are color coded as in the ribbon model, except for the grey-and-pink subunit, which has been excised to expose the turret chamber. The arrow indicates the direction in which the nascent mRNA chain is extruded through the central bore of the turret, past the enzymatic active sites that generate its 5' cap (enzyme domains: g, guanylyltransferase; m1, methyltransferase 1; m2, methyltransferase 2). S-adenosyl-L-homocysteine by-product molecules bound within the active sites of methyltransferases m1 and m2 are shown as red and yellow balls, respectively. One arm of the pentameric lid that can open in ISVPs and cores by rotating upward and outward is designated by the angle-and-arrow symbol placed above it. Ribbon models in (a) and (b) are approximately to scale. All models were rendered in PyMol (<http://www.pymol.org>).

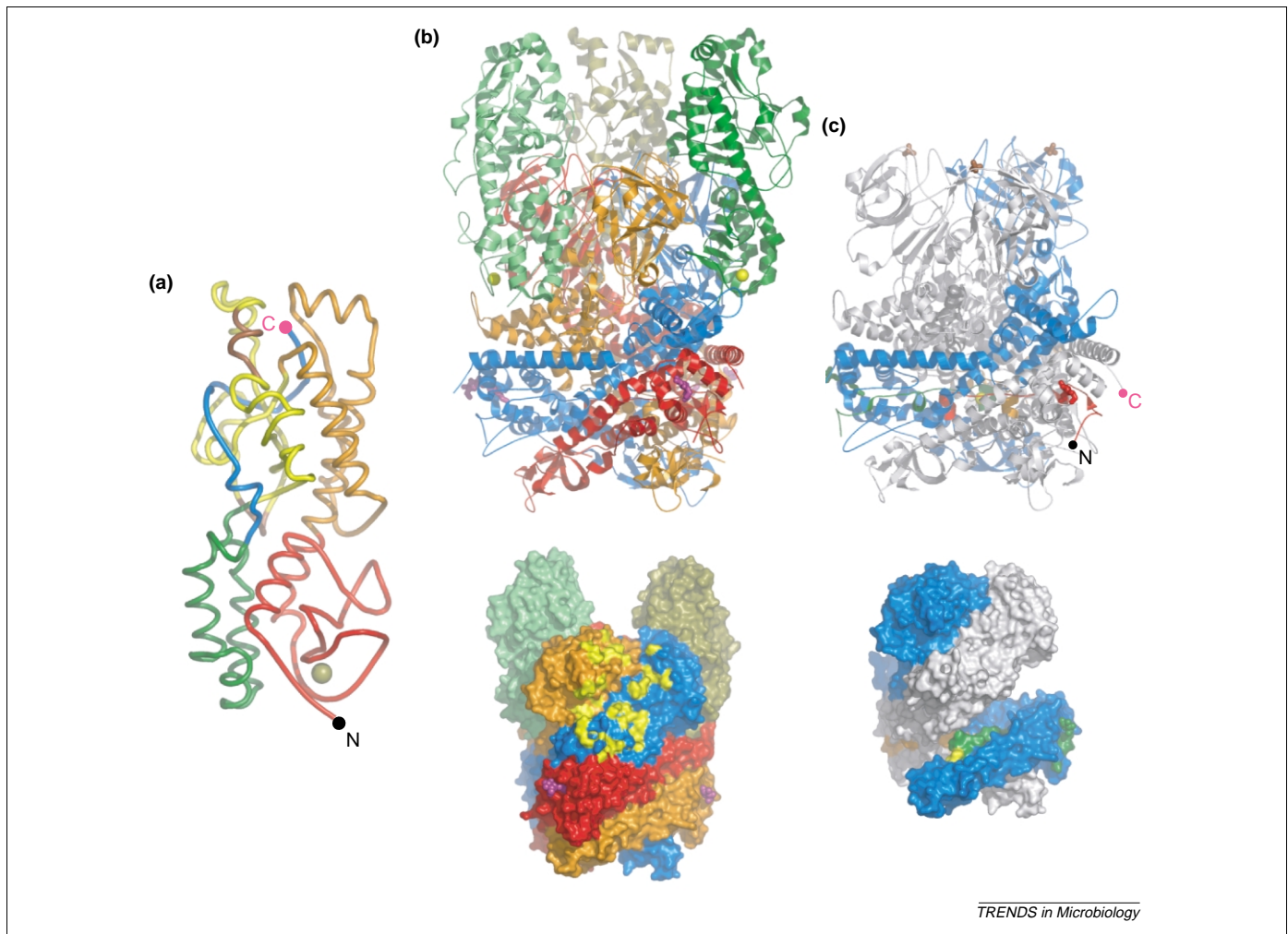
are highly infectious (commonly enhanced more than 10^6 -fold over cores). Several groups are therefore using recoated particles that contain mutant forms of recombinant $\mu 1$, $\sigma 3$ and/or $\sigma 1$ to study cell invasion [11,16–19]. Over the course of such studies, it has become clear that there is a distinct advantage of using 'recoating genetics' rather than a reverse-genetics system in which mutations are made in the genome: it allows one to study mutations with lethal effects on invasion, without the need for complementing cell lines to rescue the otherwise noninfectious clones. Similar recoating strategies will no doubt be useful for genetic studies of cell invasion by other *Reoviridae* members, including the pathogenic human rotaviruses [20].

The preceding genetic approach has been made more effective by reports of X-ray crystal structures of the delivery system proteins $\mu 1$, $\sigma 3$ and $\sigma 1$ [12,13,21]

(Figs. 2 and 3; Table 1). The structures, in addition to suggesting new ideas about the functions of these proteins, allow mutations to be designed in a rational manner, to test hypotheses about cell invasion and outer-capsid assembly. X-ray crystal structures of four of the five payload (core) proteins (e.g., $\lambda 2$ in Fig. 2) have also been recently reported [9,22] (Table 1). Coupled with systems for assembling core-like particles [23,24], the structures allow similar studies of payload function and assembly, as indicated above for the delivery system.

Steps in invasion

Cell invasion by viruses is a multi-step process. For reovirus, these steps include (1) attachment to cell surface receptors, (2) uptake into endocytic vacuoles, (3) proteolytic priming of the penetration machinery, (4) membrane



TRENDS in Microbiology

Fig. 3. Structural features of outer-capsid proteins $\sigma 3$ and $\mu 1$. (a) Side view of a $\sigma 3$ monomer extracted from the $\mu 1_3$ - $\sigma 3_3$ heterohexamer [13] and rendered as a backbone model. N and C termini are marked. The 'S' path of the backbone is highlighted by color coding according to sequence position: residues 1 to 90, red; 91 to 180, orange; 181 to 285, yellow; 285 to 335, green; and 336 to 365, aquamarine. Two hypersensitive regions for initial cleavages during proteolytic processing [17] are in the yellow region and are color coded in brown. A Zn^{2+} ion (yellow sphere) is bound within the red region. (b) Side views of the $\mu 1_3$ - $\sigma 3_3$ heterohexamer rendered as ribbon (top) or surface-shaded (bottom) models. The right side of the ribbon model has been rotated by $\sim 90^\circ$ toward the viewer to yield the view in the surface-shaded model. $\mu 1$ subunits are color coded in aquamarine, orange and red, and $\sigma 3$ subunits are color coded in shades of green. The middle/rear $\sigma 3$ in the ribbon model is in the same orientation as that in (a). A β -octylglucoside detergent molecule (purple sticks) occupies a hydrophobic, putative myristoyl-binding, pocket in each $\mu 1$ monomer. Each $\sigma 3$ monomer binds a Zn^{2+} ion (yellow sphere) within a $\mu 1$ -interacting zinc finger motif. One $\sigma 3$ subunit has been excised from the surface-shaded model, and the residues in $\mu 1$ that contact it have been color coded in yellow to illustrate the manner in which each $\sigma 3$ subunit 'tapes' across the upper parts of two adjacent $\mu 1$ subunits. (c) Side views of a $\mu 1$ trimer ($\sigma 3$ excised for clarity) rendered as ribbon (top) or surface-shaded (bottom) models. The left side of the ribbon model has been rotated by $\sim 90^\circ$ toward the viewer to yield the view in the surface-shaded model. One $\mu 1C$ subunit (residues 43 to 675) is color coded in aquamarine to illustrate its path through the trimer. The $\mu 1N$ subunits (residues 10 to 42), together with the β -octylglucoside detergent molecules (sticks) that might correspond to their N-terminal myristoyl groups, are color coded in green, orange and red (the green $\mu 1N$ subunit corresponds to the aquamarine $\mu 1C$ subunit). The approximate positions of the first and last residues visualized in the heterohexamer structure (residues 10 and 675) are respectively indicated with a black and pink circle for one of the gray-colored $\mu 1N/\mu 1C$ monomers. A pocket within the jelly-roll top domain of each $\mu 1C$ subunit that has bound a sulfate ion (brown sticks) in the crystal could represent a binding site for a membrane phospholipid. In the surface-shaded model, one $\mu 1$ subunit has been excised to more clearly illustrate the path of $\mu 1N$ through the trimer and to reveal the central location of the $\mu 1N/\mu 1C$ cleavage site (the first $\mu 1C$ residue, 43, is color coded in yellow). Ribbon models in (a) and (b) are approximately to scale. All models were rendered in PyMol (<http://www.pymol.org>).

penetration and (5) derepression of the viral transcriptases (Fig. 4). Interactions with specific host factors and trafficking between different vacuolar compartments are likely to accompany these steps. In addition, each of these steps might be further divided into substeps that could vary or be bypassed in certain cell types or at certain stages of infection in host animals. A review of steps (1) and (2) is beyond the scope of this article but has been partially supplied by other recent articles [25,26]. The remainder of this review will focus on the later steps in invasion.

Proteolytic processing primes the delivery system

Many enveloped and nonenveloped animal viruses that must undergo uptake into endocytic compartments use

acidic pH as a trigger for protein conformational changes related to membrane fusion or penetration [27–29]. These viruses are generally thought to be in a 'race' to avoid inactivation by the acid-dependent proteases active in late endosomes and lysosomes. In contrast to the acid-triggered viruses, reovirus virions must seek out, not avoid, exposure to endo/lysosomal proteases, to be activated for membrane penetration following degradation of $\sigma 3$ [30,31]. Recent studies have used selective protease inhibitors and mutant cells to demonstrate important roles for certain endo/lysosomal proteases (cysteinyll cathepsins B and L [32–34]), and minimal roles for others (aspartyl cathepsin D [35,36]), in several cell lines. The effects that the different sets (or levels) of protease

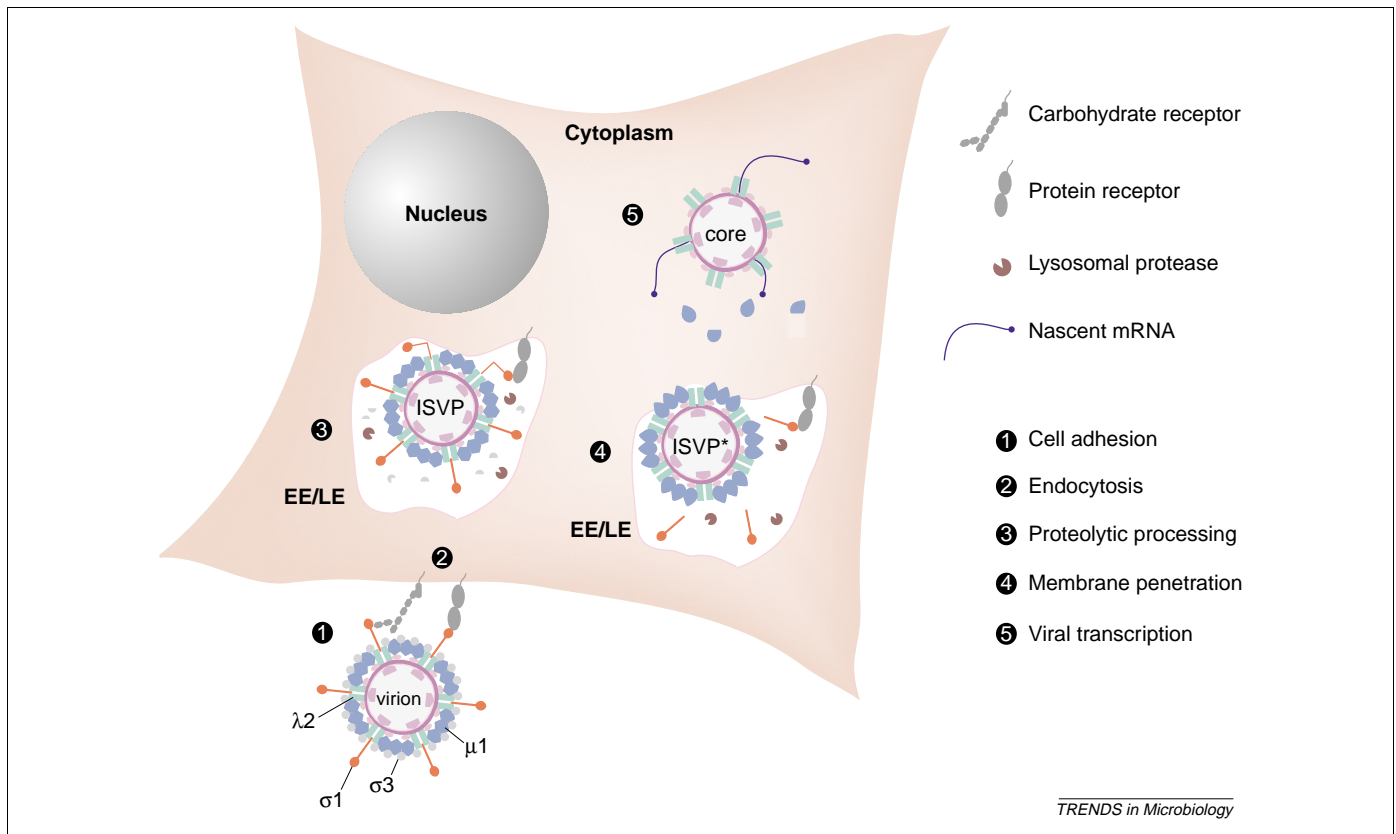


Fig. 4. Model for cell invasion. (1) Reovirus virions adhere to the cell surface by interactions between adhesin $\sigma 1$ and its carbohydrate and/or protein receptors [63]. (2) Bound virions undergo uptake into early endocytic vacuoles via one or more pathways that could require receptor(s), clathrin and dynamin [31,64]. (3) Degradation of protein $\sigma 3$ by one or more acid-dependent endo/lysosomal proteases within endocytic vacuoles converts virions to intermediate subviral particle (ISVP)-like particles. (4) The proteolytic processing of viral particles primes them for penetration of a cellular (possibly vacuolar) membrane (see text). This step is preceded by a concerted set of remodeling events induced by a putative cellular trigger factor: $\mu 1$ is converted to a hydrophobic conformer, $\mu 1^*$, and deploys the hydrophobic N-terminally myristoylated $\mu 1N$ peptide; the $\lambda 2$ turret changes conformation, releasing $\sigma 1$ from the particle; and the particle-bound viral transcriptases are derepressed. The mechanism of membrane penetration is poorly understood but is proposed to involve insertion of $\mu 1$ sequences into the target lipid bilayer. (5) The viral payload delivered into the cytoplasm could resemble either ISVP's or cores. Either type of viral particle is competent to synthesize translatable viral mRNAs using substrates from the host and the particle-bound dsRNA genome segments as templates [40]. Abbreviations: EE, early endosome; LE, late endosome.

activities in different tissues might have on viral tropism, spread and disease in animals are so far unknown [37].

$\sigma 3$ behaves as though it is designed for degradation during invasion of cells. Because other proteins in reovirus virions are largely protease-resistant, the distinctive behavior of $\sigma 3$ is striking. How might its structure determine this property? Crystal structures of $\sigma 3$ [21] and the $\mu 1_3$ - $\sigma 3_3$ heterohexamers [13] (Fig. 3) show that $\sigma 3$ has an elongated profile, perpendicular to the virion surface, with a constriction near the middle that gives it a peanut shape. The N and C termini lie near the lower and upper ends of the peanut, respectively, but the polypeptide chain traces a circuitous 'S' between the termini so that both lobes receive contributions from both halves of the protein sequence. Defined sequence determinants for degradation are located in the upper lobe or constriction. Analyses of $\sigma 3$ fragments generated by diverse proteases *in vitro* and by endo/lysosomal proteases in cells have shown that nearly all these proteases initiate cleavage within small 'hypersensitive regions' in solvent-exposed loops or arches [17,34,38] (Fig. 3). Subsequent cleavages proceed on either side of the hypersensitive regions and might be accompanied by conformational changes that render other portions of $\sigma 3$ more susceptible to cleavages [38]. The 'S' path of the polypeptide chain might facilitate

such a disassembly cascade by regularly juxtaposing sequences from distant parts of the chain. Interestingly, amino acid changes that enhance or reduce the sensitivity of $\sigma 3$ to different proteases are not located directly within the hypersensitive regions but instead modulate the cleavability of these regions through adjacent or longer-range interactions [17,19]. These features of $\sigma 3$ might provide the virus with an evolutionary advantage by allowing it to tune $\sigma 3$ degradability to suit different protease-rich and -poor environments.

$\sigma 3$ coat is a removable protective shield

The need for $\sigma 3$ degradation during invasion prompts the question: 'Why is this protein present in viral particles?' The answer appears to have at least two parts. First, $\sigma 3$ binds $\mu 1$ in solution and plays a critical role in $\mu 1$ folding and incorporation into virions [16]. Thus, $\sigma 3$ acts as a chaperone for assembling the penetration protein, similar to the accessory protein prM for the flavivirus fusion protein [39]. Unlike prM, however, intact $\sigma 3$ remains present in mature virions. The second part relates to an observation that $\sigma 3$ enhances the resistance of particles to loss of infectivity over a range of temperatures [15,18]. Protein $\mu 1$ has been identified as the key determinant of thermal inactivation of ISVPs [18], suggesting that $\sigma 3$

exerts its thermostabilizing effect through its interactions with $\mu 1$ in virions [13]. These interactions are extensive and appear to stabilize each $\mu 1$ trimer with three pieces of $\sigma 3$ 'tape', each of which spans an interface between two $\mu 1$ monomers (Fig. 3). Interestingly, the biochemical hallmarks of thermal inactivation *in vitro* (rearrangements in $\mu 1$, $\lambda 2$ and $\sigma 1$) resemble changes at physiological temperature that precede or accompany penetration of a cellular membrane during invasion (see below), and both sets of changes are blocked by the presence of $\sigma 3$ [18,40]. These findings support the idea that $\sigma 3$ acts as a protective shield for the delivery system. Its presence might prevent inappropriate, possibly catastrophic, triggering of the invasion program while viral particles are still inside the parent cell, and its removal by proteases is then required to prime the particles for invasion of new cells. The enhanced stability conferred by $\sigma 3$ also suggests that it plays a role in survival of particles outside cells and hosts. In this sense, the $\sigma 3$ layer is analogous to a bacterial spore coat that protects the dormant organism from environmental insult, yet acts as a sensor for molecules that trigger its own disassembly and spore (or virus) germination.

***In vitro* membrane permeabilization and accompanying structural changes**

In vitro assays for membrane permeabilization have proven useful for studies of membrane fusion or penetration by several different viruses [41–43]. Reovirus ISVPs, but not virions or cores, can induce permeabilization of natural and synthetic membranes to ions, small molecules and proteins [40,44–47]. These observations suggest a specific role for the ISVP in membrane penetration during cell invasion and also suggest that one or both proteins lost between ISVP and core, $\mu 1$ and $\sigma 1$, is essential for membrane permeabilization. By assaying release of hemoglobin from erythrocytes (hemolysis), it was recently shown that $\mu 1$ is the primary determinant of strain differences in the rate of membrane permeabilization [40], consistent with previous results from a ^{51}Cr -release assay [45,48]. Moreover because recoated particles devoid of $\sigma 1$ are effective at hemolysis once $\sigma 3$ is removed [11], $\sigma 1$ appears to play no direct role in membrane permeabilization. These and other observations (see below), together with structural features of $\mu 1$, such as its N-terminal myristoyl group [49], suggest that $\mu 1$ is the reovirus penetration protein.

Membrane penetration by nonenveloped virus penetration proteins might be assumed to involve insertion of hydrophobic moieties into the lipid bilayer. $\mu 1$, present in 600 copies at the ISVP surface, is ideally located to interact with target membrane. Nonetheless, ISVPs are hydrophilic particles that remain dispersed in aqueous media. Studies were carried out to test the hypothesis that $\mu 1$, like other viral fusion/penetration proteins and protein toxins that can exist in both free and membrane-bound states, must change conformation before membrane insertion. These experiments confirmed that the $\mu 1$ conformer in ISVPs can rearrange into a protease-sensitive, hydrophobic, presumptively membrane-seeking conformer, ' $\mu 1^*$ ', which is required for hemolysis [40]. In fact, the

$\mu 1 \rightarrow \mu 1^*$ conformational change is only one of a concerted set of remodeling events. Changes in $\mu 1$ are accompanied by release of adhesin $\sigma 1$ into solution, a putative conformational change in $\lambda 2$ that allows $\sigma 1$ release and derepression of the core-associated viral transcriptases. These findings led to the proposal of a modified invasion model in which the ISVP is only a precursor to an 'ISVP^{*}'-like particle that initiates membrane penetration [40] (Fig. 4). ISVP^{*}s are likely to be equivalent to the flocculated and transcriptionally active ISVPs described in older papers [50,51]. Release of $\sigma 1$ in concert with $\mu 1$ conformational changes could be an important feature of the penetration process, allowing the $\sigma 1$ fiber not to interpose between $\mu 1$ and membrane. Adenovirus is also known to shed its adhesin fiber, which shows structural and functional similarities to $\sigma 1$ [26], during penetration-related conformational changes [52]. Discussion of how the viral transcriptases become activated at the ISVP \rightarrow ISVP^{*} transition is beyond the scope of this review but this observation suggests that the particles are ready to begin transcribing, capping and exporting the viral mRNAs [9] soon after they gain access to the cytoplasm.

ISVPs are irreversibly converted to ISVP^{*}-like particles in a temperature-dependent manner that obeys first-order kinetics and the Arrhenius equation [18]. Thus, ISVPs, like the cleavage-activated proteins of many enveloped viruses (e.g. influenza virus [53]) and other nonenveloped viruses (e.g. poliovirus [54]), are metastable, i.e. trapped in a non-minimum energy state by an activation barrier that can be overcome by input of sufficient energy. The implication is that the ISVP is poised to convert to the ISVP^{*} during invasion and could be promoted or triggered to do so by a host cell factor (ion, lipid, protein, etc.) or set of conditions that it encounters along the invasion pathway. Because $\mu 1$ is the determinant of strain differences in ISVP thermostability [18,48] and undergoes major rearrangements at the ISVP \rightarrow ISVP^{*} transition (see above), it appears to be the metastable element that determines the kinetics of this transition. It is also a strong candidate to interact with any putative 'trigger factor' during invasion. Sulfate-binding sites in the $\mu 1$ top domain (see below) have been proposed as binding sites for phospholipid head groups [13], suggesting the possibility of a lipid trigger. Increased concentrations of K^+ , which promote the ISVP \rightarrow ISVP^{*} transition *in vitro* [40,55], could also contribute to the physiological triggering mechanism. Changes in Ca^{2+} concentration are known to influence rotavirus penetration [56,57].

Mutations in $\mu 1$ link *in vitro* properties to steps in cell invasion

The importance of the ISVP \rightarrow ISVP^{*} transition and the metastable nature of $\mu 1$ for membrane penetration during infection has been demonstrated with $\mu 1$ mutants in native or recoated particles. Viral strains selected for resistance to ethanol or heat inactivation contain determinative mutations in their $\mu 1$ proteins [48,58] (J.K. Middleton *et al.*, unpublished). The thermostable ISVPs of these mutants show kinetic defects in *in vitro* conversion to ISVP^{*}s, membrane permeabilization and, in some cases, invasion of cultured

cells [48] (K. Chandran *et al.*, unpublished; J.K. Middleton *et al.*, unpublished). The reduced propensity of some of these mutants to penetrate membranes during invasion suggests that the size of the activation barrier for the ISVP \rightarrow ISVP* transition might be optimized by evolution to a range of values that permits assembly of stable, but not too stable, particles, which can resist inactivation in nature but exhibit appropriate conformational lability when the time for penetration arrives [18]. Examination of several other μ 1 mutants in recoated particles has provided further evidence for the role of μ 1 in penetration (see below). One other study has identified a viral mutant that is poorly infectious, accumulates in lysosomes during cell invasion and has one or more mutations in μ 1 that determine these phenotypes [59].

How does μ 1 fulfill its role as the penetration protein? The structures of the μ 1, μ 1*, and other intermediate or downstream conformers will be required to make a 'molecular movie' of membrane penetration. Nonetheless, the recent crystal structure determination of the μ 1₃- σ 3₃ heterohexamer [13] (Fig. 3), which is similar to the complexes of these proteins found in virions, represents important progress toward that goal. The three μ 1 subunits in this conformer form an intertwined trimer comprising a mainly α -helical body and a top domain formed by three jelly-roll β -barrels. Many μ 1 mutations that cause increased thermostability and affiliated defects in membrane permeabilization by slowing the μ 1 \rightarrow μ 1* transition (see above) are located at intra- and inter-trimer interfaces between the top domains, suggesting that the μ 1 conformational changes include some dissociation of the trimer [13]. This hypothesis is also consistent with the idea that σ 3 blocks μ 1 conformational changes by 'taping' across the upper portions of the μ 1 trimer (Fig. 3).

Another likely element of the μ 1 \rightarrow μ 1* transition is release of the autolytically generated hydrophobic μ 1N peptide (N-terminal myristoyl group plus amino acids 2 to 42). The myristoyl group and first nine amino acids of μ 1N are disordered and not visible in the μ 1₃- σ 3₃ structure, possibly because the myristoyl group has been displaced from a hydrophobic pocket on the outer surface of μ 1 by a detergent molecule in the crystal [13]. From the putative myristoyl-binding pocket in the μ 1 structure, the μ 1N chain plunges laterally into the heart of the trimer, terminating near the threefold axis at the autolytic cleavage site that separates it from the rest of the molecule, μ 1C (Fig. 3). Recent experiments with recoated particles containing a μ 1 mutant that is not cleaved at the μ 1N/ μ 1C junction have indicated that these particles are poorly infectious, fail to mediate hemolysis once σ 3 is removed, and are defective at penetrating into the cytoplasm and initiating viral protein synthesis (A.L. Odegard *et al.*, unpublished). Thus, autocleavage and/or release of μ 1N is likely to be required for membrane penetration.

Penetration mechanism

How might the proposed structural changes promote μ 1-bilayer interactions? The myristoylated μ 1N peptide is a prime candidate to insert into the target membrane. Rearrangement and membrane insertion of apolar or

amphipathic α -helices previously buried inside the μ 1 trimer (Fig. 3) also seem likely, given the enhanced sensitivity of sequences in this region to trypsin cleavage in the μ 1* conformer and observations that their proteolytic removal from ISVP*s blocks hemolysis (μ 1N is not expected to be cleaved by trypsin) [40]. This model for penetration-related changes is similar to that proposed for poliovirus. In poliovirus, an autolytic cleavage results in deployment of an N-terminally myristoylated peptide, VP4, which, together with an amphipathic α -helical bundle from a region of the capsid in VP1, is thought to insert into the target membrane [6]. The penetration mechanisms of reovirus and poliovirus might diverge after these initial steps, however, considering their distinct payloads (700 Å icosahedral particle versus RNA chain, respectively).

The preceding discussions make clear that there is still much to learn about the way in which μ 1 changes conformation and inserts into a membrane. Even less is known about the intra-bilayer structures formed by μ 1 sequences and how these could promote cytoplasmic delivery of the oversized payload. Large (>200 Å) protein-lined pores analogous to those formed by bacterial cholesterol-dependent cytolysins (e.g., streptolysin-O [60]) are one possibility. Production of multiple pores within the membrane of an endocytic compartment could facilitate the disruption and release of particles into the cytoplasm, as suggested to occur for bacteria that secrete such toxins. Alternatively, ISVP*s (and/or released μ 1N) could disrupt the membrane by forcing the lipids into non-bilayer structures, in the same way as detergent micelles, as occurs with some other toxins (e.g., magainin [61]). The scarcity of data allows the possibility of other scenarios, however, such as membrane insertion of a patch of μ 1 subunits, followed by lateral diffusion of the entire μ 1 layer into the lipid bilayer and coupled release of the core into the cytoplasm. This model resembles the penetration of filamentous f1 bacteriophages into their bacterial hosts [62]. More advanced studies will be necessary to distinguish between these and other conceivable mechanisms.

Cell biology of invasion

The cell biology of invasion by reovirus remains poorly characterized. Although it is thought that virions are removed from the cell surface by receptor-mediated endocytosis, that ISVP-like particles are generated by proteolysis within late endosomes or lysosomes, and that the particles then penetrate into the cytoplasm from those vacuoles, there is little direct evidence to support those conclusions. For infection initiated by ISVPs, it is thought that penetration could occur at the plasma membrane, but, again, there is limited evidence to support this conclusion. With the availability of newer and better methods to visualize viral particles within cellular substructures and to manipulate cellular pathways either genetically or biochemically, this is expected to be a productive area of research in the next few years.

Concluding remarks

Recent advances in understanding how reoviruses cross a host cell membrane during invasion have been propelled

Questions for Future Research

- Is there a trigger factor for $\mu 1$ to initiate membrane penetration, and what is this factor?
- What regions of $\mu 1N$ and/or $\mu 1C$ insert into the target membrane, which of these are required for membrane penetration, and what structures do the inserted regions adopt?
- What is the general mechanism of payload translocation: through a large trans-membrane pore – through a disruptive perforation, or by other means?
- From which subcellular compartment does membrane penetration occur, and is there a difference when infection is initiated by a virion versus an ISVP?
- Is $\mu 1C$ removed from the core during or after membrane penetration?
- Is release of the $\sigma 1$ adhesin fibers required for membrane penetration, and do the released fibers play any other role?

by new X-ray crystal structures of delivery system proteins (Table 1); a new genetic technology, recoating, which allows dissection of the cell invasion mechanisms from the ‘virus side’; and studies of programmed changes in particle structure which precede membrane permeabilization *in vitro*. The emerging picture suggests that proteolytic degradation of protector protein $\sigma 3$ primes particles to undergo the dramatic structural transition required for membrane penetration and activation of viral mRNA synthesis. Key components of this transition include conformational changes in penetration protein $\mu 1$, which is likely to permit insertion of $\mu 1$ regions into the host membrane, and shedding of adhesin $\sigma 1$. The findings discussed in this review should fuel future work on the membrane penetration problem (Questions for Future Research) along four overlapping fronts: (1) further biochemical and structural descriptions of particle/protein invasion intermediates; (2) translation of *in vitro* findings into infection models using cell biological assays in conjunction with mutant viral particles; (3) identification of host cell factors involved in invasion; and (4) characterization of virus–membrane interactions. It is anticipated that progress on understanding cell invasion by reoviruses will also illuminate the mechanisms used by other large nonenveloped viruses to enter their host cells.

Acknowledgements

We thank T.S. Baker, S.C. Harrison, T. Kirchhausen, J.K. Middleton, L.A. Schiff and J. Yin for helpful discussions. We also thank T.J. Broering, I. S. Kim, K.S. Myers, A.L. Odegard, J.S.L. Parker and other members of our laboratory for helpful discussions or critiques. We apologize to colleagues whose work may not have been cited due to length constraints. Work on reovirus invasion and mRNA synthesis is supported in our laboratory by United States Public Health Service grants AI46440 and AI47904 from the NIH.

References

- 1 Nibert, M.L. *et al.* (1991) Mechanisms of viral pathogenesis. Distinct forms of reoviruses and their roles during replication in cells and host. *J. Clin. Invest.* 88, 727–734
- 2 Skehel, J.J. and Wiley, D.C. (2000) Receptor binding and membrane fusion in virus entry: the influenza hemagglutinin. *Annu. Rev. Biochem.* 69, 531–569
- 3 Harrison, S.C. (2001) Principles of virus structure. In *Fields Virology* (Knipe, D.M. and Howley, P.M., eds), pp. 53–85, Lippincott Williams & Wilkins
- 4 Heinz, F.X. and Allison, S.L. (2001) The machinery for flavivirus fusion with host cell membranes. *Curr. Opin. Microbiol.* 4, 450–455
- 5 Schneemann, A. *et al.* (1998) The structure and function of nodavirus particles: a paradigm for understanding chemical biology. *Adv. Virus Res.* 50, 381–446
- 6 Hogle, J.M. (2002) Poliovirus cell entry: common structural themes in viral cell entry pathways. *Annu. Rev. Microbiol.* 56, 677–702
- 7 Nibert, M.L. and Schiff, L.A. (2001) Reoviruses and their replication. In *Fields Virology* (Knipe, D.M. and Howley, P.M., eds), pp. 1679–1728, Lippincott Williams & Wilkins
- 8 Estes, M.K. (2001) Rotaviruses and their replication. In *Fields Virology* (Knipe, D.M. and Howley, P.M., eds), pp. 1679–1728, Lippincott Williams & Wilkins
- 9 Reinisch, K.M. *et al.* (2000) Structure of the reovirus core at 3.6 Å resolution. *Nature* 404, 960–967
- 10 Luongo, C.L. *et al.* (2000) Identification of the guanylyltransferase region and active site in reovirus mRNA capping protein $\lambda 2$. *J. Biol. Chem.* 275, 2804–2810
- 11 Chandran, K. *et al.* (2001) Complete *in vitro* assembly of the reovirus outer capsid produces highly infectious particles suitable for genetic studies of the receptor-binding protein. *J. Virol.* 75, 5335–5342
- 12 Chappell, J.D. *et al.* (2002) Crystal structure of reovirus attachment protein $\sigma 1$ reveals evolutionary relationship to adenovirus fiber. *EMBO J.* 21, 1–11
- 13 Liemann, S. *et al.* (2002) Structure of the reovirus membrane-penetration protein, $\mu 1$, in a complex with its protector protein, $\sigma 3$. *Cell* 108, 283–295
- 14 Dryden, K.A. *et al.* (1993) Early steps in reovirus infection are associated with dramatic changes in supramolecular structure and protein conformation: analysis of virions and subviral particles by cryoelectron microscopy and image reconstruction. *J. Cell Biol.* 122, 1023–1041
- 15 Jane-Valbuena, J. *et al.* (1999) Reovirus virion-like particles obtained by recoating infectious subvirion particles with baculovirus-expressed $\sigma 3$ protein: an approach for analyzing $\sigma 3$ functions during virus entry. *J. Virol.* 73, 2963–2973
- 16 Chandran, K. *et al.* (1999) *In vitro* recoating of reovirus cores with baculovirus-expressed outer-capsid proteins $\mu 1$ and $\sigma 3$. *J. Virol.* 73, 3941–3950
- 17 Jane-Valbuena, J. *et al.* (2002) Sites and determinants of early cleavages in the proteolytic processing pathway of reovirus surface protein $\sigma 3$. *J. Virol.* 76, 5184–5197
- 18 Middleton, J.K. *et al.* (2002) Thermostability of reovirus disassembly intermediates (ISVPs) correlates with genetic, biochemical, and thermodynamic properties of major surface protein $\mu 1$. *J. Virol.* 76, 1051–1061
- 19 Wilson, G.J. *et al.* (2002) A single mutation in the carboxy terminus of reovirus outer-capsid protein $\sigma 3$ confers enhanced kinetics of $\sigma 3$ proteolysis, resistance to inhibitors of viral disassembly, and alterations in $\sigma 3$ structure. *J. Virol.* 76, 9832–9843
- 20 Chen, D. and Ramig, R.F. (1993) Rescue of infectivity by *in vitro* transcapsidation of rotavirus single-shelled particles. *Virology* 192, 422–429
- 21 Olland, A.M. *et al.* (2001) Structure of the reovirus outer capsid and dsRNA-binding protein $\sigma 3$ at 1.8 Å resolution. *EMBO J.* 20, 979–989
- 22 Tao, Y. *et al.* (2002) RNA synthesis in a cage – structural studies of reovirus polymerase $\lambda 3$. *Cell* 111, 733–745
- 23 Xu, P. *et al.* (1993) Generation of reovirus core-like particles in cells infected with hybrid vaccinia viruses that express genome segments L1, L2, L3, and S2. *Virology* 197, 726–731
- 24 Kim, J. *et al.* (2002) The hydrophilic amino-terminal arm of reovirus core shell protein $\lambda 1$ is dispensable for particle assembly. *J. Virol.* 76, 12211–12222
- 25 Tyler, K.L. *et al.* (2001) Reoviruses and the host cell. *Trends Microbiol.* 9, 560–564
- 26 Stehle, T. and Dermody, T.S. (2003) Structural evidence for common functions and ancestry of the reovirus and adenovirus attachment proteins. *Rev. Med. Virol.* 13, 123–132
- 27 Mothes, W. *et al.* (2000) Retroviral entry mediated by receptor priming and low pH triggering of an envelope glycoprotein. *Cell* 103, 679–689
- 28 White, J. *et al.* (1981) Cell fusion by Semliki Forest, influenza, and vesicular stomatitis viruses. *J. Cell Biol.* 89, 674–679
- 29 Brabec, M. *et al.* (2003) Conformational changes, plasma membrane penetration, and infection by human rhinovirus type 2: role of receptors and low pH. *J. Virol.* 77, 5370–5377

- 30 Sturzenbecker, L.J. *et al.* (1987) Intracellular digestion of reovirus particles requires a low pH and is an essential step in the viral infectious cycle. *J. Virol.* 61, 2351–2361
- 31 Martinez, C.G. *et al.* (1996) The entry of reovirus into L cells is dependent on vacuolar proton-ATPase activity. *J. Virol.* 70, 576–579
- 32 Baer, G.S. and Dermody, T.S. (1997) Mutations in reovirus outer-capsid protein $\sigma 3$ selected during persistent infections of L cells confer resistance to protease inhibitor E64. *J. Virol.* 71, 4921–4928
- 33 Baer, G.S. *et al.* (1999) Mutant cells selected during persistent reovirus infection do not express mature cathepsin L and do not support reovirus disassembly. *J. Virol.* 73, 9532–9543
- 34 Ebert, D.H. *et al.* (2002) Cathepsin L and cathepsin B mediate reovirus disassembly in murine fibroblast cells. *J. Biol. Chem.* 277, 24609–24617
- 35 Kothandaraman, S. *et al.* (1998) No role for pepstatin-A-sensitive acidic proteinases in reovirus infections of L or MDCK cells. *Virology* 251, 264–272
- 36 Ebert, D.H. *et al.* (2001) Adaptation of reovirus to growth in the presence of protease inhibitor E64 segregates with a mutation in the carboxy terminus of viral outer-capsid protein $\sigma 3$. *J. Virol.* 75, 3197–3206
- 37 Golden, J.W. *et al.* (2002) Addition of exogenous protease facilitates reovirus infection in many restrictive cells. *J. Virol.* 76, 7430–7443
- 38 Mendez, I. *et al.* Structure of the reovirus outer capsid and kinetics of its digestion as determined by mass spectrometry. *Virology* (in press)
- 39 Lorenz, I.C. *et al.* (2002) Folding and dimerization of tick-borne encephalitis virus envelope proteins prM and E in the endoplasmic reticulum. *J. Virol.* 76, 5480–5491
- 40 Chandran, K. *et al.* (2002) Strategy for nonenveloped virus entry: a hydrophobic conformer of reovirus penetration protein $\mu 1$ mediates membrane disruption. *J. Virol.* 76, 9920–9933
- 41 Blumenthal, R. *et al.* (1986) pH dependent lysis of liposomes by adenovirus. *Biochemistry* 25, 2231–2237
- 42 Nandi, P. *et al.* (1992) Interaction of rotavirus particles with liposomes. *J. Virol.* 66, 3363–3367
- 43 Lenard, J. and Miller, D.K. (1981) pH-dependent hemolysis by influenza, Semliki, Forest virus, and Sendai virus. *Virology* 110, 479–482
- 44 Borsa, J. *et al.* (1979) Two modes of entry of reovirus particles into L cells. *J. Gen. Virol.* 45, 161–170
- 45 Lucia-Jandris, P. *et al.* (1993) Reovirus M2 gene is associated with chromium release from mouse L cells. *J. Virol.* 67, 5339–5345
- 46 Tosteson, M.T. and Chow, M. (1997) Characterization of the ion channels formed by poliovirus in planar lipid membranes. *J. Virol.* 71, 507–511
- 47 Chandran, K. and Nibert, M.L. (1998) Protease cleavage of reovirus capsid protein $\mu 1/\mu 1C$ is blocked by alkyl sulfate detergents, yielding a new type of infectious subviral particle. *J. Virol.* 72, 467–475
- 48 Hooper, J.W. and Fields, B.N. (1996) Role of the $\mu 1$ protein in reovirus stability and capacity to cause chromium release from host cells. *J. Virol.* 70, 459–467
- 49 Nibert, M.L. *et al.* (1991) Mammalian reoviruses contain a myristoylated structural protein. *J. Virol.* 65, 1960–1967
- 50 Joklik, W.K. (1972) Studies on the effect of chymotrypsin on reovirions. *Virology* 49, 700–715
- 51 Shatkin, A.J. and LaFiandra, A.J. (1972) Transcription by infectious subviral particles of reovirus. *J. Virol.* 10, 698–706
- 52 Nakano, M. *et al.* (2000) The first step of adenovirus type 2 disassembly occurs at the cell surface, independently of endocytosis and escape to the cytosol. *J. Virol.* 74, 7085–7095
- 53 Carr, C.M. *et al.* (1997) Influenza hemagglutinin is spring-loaded by a metastable native conformation. *Proc. Natl. Acad. Sci. U. S. A.* 94, 14306–14313
- 54 Tsang, S.K. *et al.* (2001) Kinetic analysis of the effect of poliovirus receptor on viral uncoating: the receptor as a catalyst. *J. Virol.* 75, 4984–4989
- 55 Borsa, J. *et al.* (1974) Reovirus transcriptase activation *in vitro*: involvement of an endogenous uncoating activity in the second stage of the process. *Intervirology* 4, 171–188
- 56 Chemello, M.E. *et al.* (2002) Requirement for vacuolar H⁺-ATPase activity and Ca²⁺ gradient during entry of rotavirus into MA104 cells. *J. Virol.* 76, 13083–13087
- 57 Martin, S. *et al.* (2002) Ionic strength- and temperature-induced K(Ca) shifts in the uncoating reaction of rotavirus strains RF and SA11: correlation with membrane permeabilization. *J. Virol.* 76, 552–559
- 58 Wessner, D.R. and Fields, B.N. (1993) Isolation and genetic characterization of ethanol-resistant reovirus mutants. *J. Virol.* 67, 2442–2447
- 59 Hazelton, P.R. and Coombs, K.M. (1995) The reovirus mutant tsA279 has temperature-sensitive lesions in the M2 and L2 genes: the M2 gene is associated with decreased viral protein production and blockade in transmembrane transport. *Virology* 207, 46–58
- 60 Bhakdi, S. *et al.* (1996) Staphylococcal alpha-toxin, streptolysin-O, and *Escherichia coli* hemolysin: prototypes of pore-forming bacterial cytolysins. *Arch. Microbiol.* 165, 73–79
- 61 Shai, Y. (1999) Mechanism of the binding, insertion and destabilization of phospholipid bilayer membranes by alpha-helical antimicrobial and cell non-selective membrane-lytic peptides. *Biochim. Biophys. Acta* 1462, 55–70
- 62 Click, E.M. and Webster, R.E. (1998) The TolQRA proteins are required for membrane insertion of the major capsid protein of the filamentous phage $\phi 1$ during infection. *J. Bacteriol.* 180, 1723–1728
- 63 Barton, E.S. *et al.* (2001) Junction adhesion molecule is a receptor for reovirus. *Cell* 104, 441–451
- 64 Borsa, J. *et al.* (1981) Reovirus: evidence for a second step in the intracellular uncoating and transcriptase activation process. *Virology* 111, 191–200

TIM online – making the most of your personal subscription

High-quality printouts (from PDF files)
Links to other articles, other journals and cited software and databases

All you have to do is:

Obtain your subscription key from the address label of your print subscription.
Then go to <http://www.trends.com>, click on the **Claim online access** button and select **Trends in Microbiology**.
You will see a BioMedNet login screen. Please enter your BioMedNet username and password. If you are not a BioMedNet member already, please click on the **Join Now** button to register. You will then be asked to enter your subscription key.
Once confirmed, you have full-text access to *Trends in Microbiology*.

If you obtain an error message please contact **Customer Services** (info@current-trends.com) stating your subscription key and BioMedNet username and password. Please note that you only need to enter your subscription key once, BioMedNet will remember your subscription.

Institutional access is available at a premium.

If your institute is interested in subscribing to print and online, please ask them to contact ct.subs@qss-uk.com